Desalination and Water Treatment
www.deswater.com
doi: 10.1080/19443994.2016.1189707

57 (2016) 26641–26647
November

Taylor & Francis
Taylor & Francis Group

Influence of hydrophobic and electrostatic membrane surface properties on biofouling in a submerged membrane bioreactor under different filtration modes

Youngpil Chun[a,b], Dennis Mulcahy[a], Linda Zou[c], In S. Kim[d], Pierre Le-Clech[b,*]

[a]*Centre for Water Management and Reuse, School of Natural and Built Environments, University of South Australia, Mawson Lakes, Australia*
[b]*UNESCO Centre for Membrane Science and Technology, School of Chemical Engineering, University of New South Wales, Sydney, Australia, email: p.le-clech@unsw.edu.au (P. Le-Clech)*
[c]*Department of Chemical and Environmental Engineering, Masdar Institute of Science and Technology, Abu Dhabi, United Arab Emirates*
[d]*Global Desalination Research Center (GDRC), School of Environmental Science & Engineering, Gwangju Institute of Science and Technology (GIST), Gwangju, Republic of Korea*

Received 9 December 2015; Accepted 24 December 2015

ABSTRACT

This study investigated the effect of membrane surface properties on membrane biofouling in a submerged membrane bioreactor treating synthetic wastewater, by employing qualitative membrane surface examination techniques and biofilm quantification. The investigation was carried out on three different types of fouled membrane samples obtained using different filtration methods. Lipid phosphate concentration, which represents viable biomass, was employed as a direct measure of biofouling. Contact angle and zeta potential measurements of clean and fouled ultrafiltration and hollow fibre membranes were conducted. Zeta potentials of membrane samples were measured at various electrolyte pHs. The surface energy of membrane samples was calculated and reported from the data obtained from contact angle of measurements. The outcomes from this study can be used as the basis of a technique to examine the potential of biofouling in membrane processes.

Keywords: Submerged membrane bioreactor; Membrane biofouling; Zeta potential; Contact angle; Phospholipids analysis

1. Introduction

Membrane bioreactors (MBRs) which are combination of a suspended growth bioreactor and a membrane process are an alternative to conventional activated sludge processes for water and wastewater treatment. MBRs have been one of the strong techniques for municipal and industrial wastewater treatment with increased concerns about public health and rigorous environmental regulations [1]. With several advantages such as high biodegradation efficiency, small footprint and less sludge production, submerged MBRs (SMBRs) are increasingly used for

*Corresponding author.

Presented at the 8th International Desalination Workshop (IDW) 2015, November 18–21, 2015, Jeju Island, Korea

biological wastewater treatment. However, due to their configuration, membranes used for SMBRs are prone to cause fouling as a result of interaction with sludge and mixed liquor [2]. Colloids and particulate matter are considered to cause the most fouling in membrane systems [3]. However, biofouling is thought to be a major problem of the processes because all other foulants can be removed using various inhibitors and pretreatment techniques [4]. It has been revealed that extracellular polymeric substances (EPS) or soluble microbial products (SMP) may be considered as major biological foulants in SMBRs. They are important because of their impacts on effluent quality and treatment efficiency [5]. Biological fouling varies with the components of activated sludge characteristics, EPS, the amount of SMP, food/microorganisms (F/M) ratio and operational parameters such as solids retention time (SRT), feedwater chemistry, particle size and mixed liquor suspended solids (MLSS) concentration [6,7].

It is recognised that membrane biofouling is affected by physical and chemical properties such as surface roughness of the membrane and charge properties of the membrane surface. The examination of surface charge properties of a membrane is essential to reduce membrane fouling. These surface charge properties can be represented by the zeta potential, which is defined as the electrical potential value at the slipping plane (or slip layer) between the Stern layer and the diffuse layer [8]. In the aqueous phase, membrane surface charges depend on the chemical characteristics of membrane (e.g. functional groups of polymeric membrane such as R-COOH, R-NH_3^+ and R-SO_3H) and the chemistry of the solution [3]. In addition, even in the absence of ionisable functional groups, membrane surfaces can possess surface charges by adsorption of anions, polyelectrolytes, ionic surfactants and charged macromolecules from the solution. Zeta potential is a function of pH and ionic strength. Accordingly, changing pH could modify the localised charge of the membrane and foulants surface by alteration of total amount of charge or charge neutralisation, and it creates opportunities for chemical interaction by a non-ionic mechanism. These surface charges of membrane and solutes can be used to identify adhesive properties of foulants associate with other factors such as hydrophobicity.

It is noted that adhesion of the biofoulants is thought to be extremely complex due to their chemical, physical and physiological surface characteristics but is important to control. Thus, it would be useful to measure the work of adhesion of biofoulants onto solid surfaces in the aqueous phase. Xu et al. [9] documented adhesion properties of membranes by comparing contact angles of fouled and virgin membranes treating municipal wastewater coupled with attenuated total reflectance–Fourier transform infrared spectroscopy (ATR-FTIR) and phospholipids analyses. Various methods have been employed to identify bacterial biomass including dry weight and organic contents, protein, hydrocarbon, or humic substance assay, and DNA contents [10]. The main drawback of these methods is low repeatability and over estimation [11]. Phospholipid tests quantify the amount of phospholipids present in the cell walls of viable biomass cells. It has been reported that quantification of lipid extracts is one the most satisfactory methods in terms of not only sensitivity and stability but also accuracy and simplicity. In addition, a variety of organophosphates can be recovered in a complex matrix [12].

In this study, the electrostatic and hydrophobic interactions on membrane biofouling in a pilot-scale SMBR were investigated. Ultrafiltration (UF) and two different types of hollow fibre (HF) membranes were used under different filtration modes. Through the application of membrane surface and biofoulants characterisation techniques which include membrane surface charge and free energy, and phospholipid tests, the impact of membrane surface properties on biofouling was assessed.

2. Materials and methods

2.1. Membrane samples

PLTK cellulosic membrane (UF disk filter, Millipore, Australia) and two different types of HF membranes, namely UF, HF I (Memcor, Australia) and HF II (GE-Zenon, Australia), were used for SMBR operation, membrane surface characterisations and biomass quantification. A brief description of membrane samples used in this study is given in Table 1. Due to the unavailability of clean HF 2 membranes for comparison, fouled HF 2 membranes were soaked in MilliQ water (MilliQ™, Australia) for 24 h and washed thoroughly (named as WHF II).

2.2. Pilot-scale SMBR operation and different foulants filtration modes

The fouling experiments were conducted on a pilot-scale SMBR treating synthetic wastewater with a working volume of 22 L. The SMBR was operated using HF II membranes for nearly 3 years based on the constant flow (not the pressure), and when the pressure reached 30 kPa, the membranes were rinsed using tap water. The normal operating pressures were

Table 1
Membrane samples used in this study and their properties

Membrane	Chemistry	Properties	Filtration mode
UF	Regenerated cellulose	MWCO 30 kDa, 150 mm diameter	Passive filtration
HF I	Polyvinylidene fluoride (PVDF)	Pore size 0.04 μm, 1.3 mm outer diameter	Passive filtration
HF II	PVDF	Pore size 0.04 μm, outer diameter 1.92 mm, inner diameter 0.9 mm	Active filtration

Table 2
Operating parameters of the SMBR

Parameters	Value
Membrane surface area	0.579 cm^2
Pressure	9–15 kPa
Type of membrane	PVDF HF membranes (HF II)
Influent flow	55 mL/min
Solids retention time (SRT)	20 d
pH	5.6–7.6
DO	0.83–5.25 mg/L
MLSS	4,659–7,530 mg/L

Table 3
Chemical composition of the synthetic wastewater

Chemicals	g/8 L–MilliQ water
Glucose	126.4
Sodium acetate	101.6
Ammonium chloride	30.56
Peptone	28
Meat extract	17.2
Monobase phosphate	10.2
Magnesium chloride	8.8
Iron(II) sulphate	1.26

9–15 kPa, and detailed operating parameters are shown in Table 2. The composition of the synthetic wastewater is given in Table 3. The designated synthetic wastewater was fed with a dilution ratio of 1:100 using tap water; however, the dilution ratio slightly varied over time due to the wearing of peristaltic tubes, membrane fouling and aeration to the SMBR.

Two different filtration modes were applied. HF II membranes were used for active filtration as described above, and UF and HF I membranes were used for passive filtration. Known areas of the UF and HF I membranes were hung in the membrane bioreactor in order to obtain biofouled membrane samples. These membranes were left under immersion for 3 weeks in the SMBR with aeration. It contained synthetic biomass, the same used for the active filtration. After the fouling experiments by active and passive filtration, membrane modules and samples were taken out of the SMBR and rinsed using MilliQ water and then analysed. Membrane samples were stored in refrigerator for a recorded time or analysed directly.

2.3. Zeta potential measurements

A surface electrokinetic analyser (SurPASS, Anton Paar, Austria) was used to measure the zeta potential of clean and fouled membrane specimens. Measurements were conducted with a 10 mM KCl (Sigma–Aldrich, Australia) electrolyte solution over a range of pH from 3 to 9 using an automated titrating unit. The Fairbrother–Mastin approach [13] was used to transform potential vs. pressure data into zeta potential. Virgin membrane samples were soaked in MilliQ water for 24 h to remove leaching additives on the membranes that could possibly affect the results.

2.4. Contact angle measurements and surface energy determination

The wetting and adhesion properties of the membranes were characterised by contact angle measurement using an optical contact angle and surface tension meter (KSV CAM 200, Finland). The probe liquids were water, glycerol (polar; Sigma–Aldrich, Australia) and diiodomethane (a non-polar; Sigma–Aldrich, Australia), and their surface tensions are listed in Table 4. For UF membranes, at least ten liquid probe droplets were applied to the specimen surface and the images of droplets were recorded immediately after the droplet was deposited on the membrane surface. For HF membranes, samples were soaked in a vessel containing a liquid probe until the meniscus was stable and the liquid level was lowered. Then, images were recorded.

Surface energies of sample surfaces were evaluated using a method introduced by van Oss [15]. For a water environment, the Young–Dupre equation [16] is given by:

Table 4
Surface tension (mN/m) and its components used for contact angle measurements [14]. γ_L is surface tension of the test liquid and γ_L^{LW}, γ_L^+ and γ_L^- are its Lifshitz–van der Waals, acidic and basic components, respectively

Liquid	γ_L	γ_L^{LW}	γ_L^+	γ_L^-
Water (W)	72.8	21.8	25.5	25.5
Glycerol (G)	64	34	57.4	3.92
Diiodomethane (D)	50.8	50.8	0	0

$$(1 + \cos\theta)\gamma_L = -\Delta G_{SL} \quad (1)$$

where θ is the experimentally measured contact angle. ΔG_{SL} is the free energy of interaction at the interface between the liquid and the surface, while γ_L is the surface tension of the liquid. The free energy of interaction (ΔG_{SL}) can be divided into two components:

$$\Delta G_{SL} = \Delta G_{SL}^{LW} + \Delta G_{SL}^{AB} \quad (2)$$

where LW refers to Lifshitz–van der Waals interactions and AB refers to Lewis acid–base interactions. van Oss [15] further defined the components, ΔG_{SL}^{LW} and ΔG_{SL}^{AB} as:

$$\Delta G_{SL}^{LW} = -2\sqrt{\gamma_S^{LW}\gamma_L^{LW}} \quad (3)$$

$$\Delta G_{SL}^{AB} = -2\sqrt{\gamma_S^+\gamma_L^-} - 2\sqrt{\gamma_S^-\gamma_L^+} \quad (4)$$

which yields the extended Young–Dupre equation to illustrate the surface energy of the samples surfaces:

$$\gamma_L(1 + \cos\theta) = 2\left(\sqrt{\gamma_S^{LW}\gamma_L^{LW}} + \sqrt{\gamma_S^+\gamma_L^-} + \sqrt{\gamma_S^-\gamma_L^+}\right) \quad (5)$$

where γ_L is the surface tension of the test liquid, θ is the contact angle and γ_S is the surface free energy. In order to determine the surface free energy (γ_L^{LW}) and the values of the γ_S^+ and γ_S^- components of the solid, at least three liquid probes with known surface tension parameters (γ_L^{LW}, γ_L^+ and γ_L^-) must be used. Two of these need to be polar [17]. The total surface free energy of the solid is then given by:

$$\gamma_S = \gamma_S^{LW} + \gamma_S^{AB} \quad (6)$$

where $\gamma_S^{AB} = 2\left(\gamma_S^+ + \gamma_S^-\right)^{1/2}$. Using diiodomethane with zero values of γ_L^+ and γ_L^-, Eq. (5) reduced to:

$$\gamma_S^{LW} = \gamma_L\frac{(1 + \cos\theta)^2}{4} \quad (7)$$

After this step, γ_L^+ and γ_L^- can be determined using two different polar liquids and solving the resulting two equations.

2.5. Phospholipids analysis

Phospholipids analysis was conducted to quantify viable biomass in the membrane fouling layer with minor modifications from the methods developed by Findlay et al. [12]. Clean membrane samples and blanks containing no membrane sample were also prepared as a control. To extract phospholipids, biofouled membrane samples were mixed with a solution of MilliQ water, methanol (Sigma–Aldrich, Australia) and chloroform (Sigma–Aldrich, Australia) with a ratio of 0.8:2:1 (2 mL of MilliQ water, 5 mL of methanol and 2.5 mL of chloroform). Vials were tightly sealed and shaken vigorously for 24 h on a rotary shaker. Chloroform and 0.0306 M sulphuric acid (Sigma–Aldrich, Australia) were added to achieve a final ratio of chloroform:methanol:water of 1:1:0.9 (2.5 mL of chloroform and 2.5 ml of sulphuric acid were used). Vials were briefly mixed, and phases were allowed to separate undistributed for at least 8 h. Standards were prepared from a standard stock solution (15.3 mg of β-glycerophosphate ($C_3H_7O_6PNa_2$; Sigma–Aldrich, Australia) was dissolved in 50 mL methanol). The lower chloroform layer (4 ml) was removed by a pipette and transferred to a glass ampoule. Samples and standards were dried in a fume cupboard, and then, 0.9 mL of saturated potassium persulfate reagent (5% potassium persulfate in 0.36 N sulphuric acid) was added. The potassium persulfate reagent has to be brought to room temperature before addition. All the ampoules were shaken and sealed tightly, and the samples were digested for 8 h at 96℃ and dried at 57℃ overnight. After cooling, 0.2 mL of 2.5% ammonium molybdate (Sigma–Aldrich, Australia) was added and mixed well. After 10 min, 0.9 mL of malachite green reagent (Sigma–Aldrich, Australia) was added and allowed for 30 min to develop colour. Colour intensity, indicating the presence of organic phosphate, was determined at 610 nm by UV/vis spectroscopy (Agilent, Australia).

3. Results and discussion

3.1. Influence of membrane characteristics on membrane biofouling

3.1.1. Zeta potential

Overall, HF I and II membranes exhibited negative zeta potential values over the pH range 3–9 (Fig. 1). The UF membranes appeared to have an isoelectric point at pH 4.7. At a lower pH range than the isoelectric point, the effect of cations and H^+ could be increased near the Stern plane [8]. As pH increased, the zeta potential values became more negative due to the accumulation of anions of the electrolyte. HF II shows more negative values than the other membrane samples in the order of HF II, HF I and UF. This is probably due to different rates of ionisable functionality, effect of pore size and absorbability of a membrane. Due to the differences in pore size between UF and HF membranes, different types of ionisable functional group may exist in the pore wall. The differences in zeta potential values of clean and fouled UF and HF II were negligible or modest. However, the deposited fouling layer had a marked impact on zeta potentials of the HF I membrane. HF I membranes are more negatively charged over the range of pH than UF membranes under the same filtration mode. This may be attributed to the presence of organics affecting the results or accumulation of charged foulants over the range of pH.

In the case of a more negatively charged membrane, bacteria and colloids which are net negatively charged are expected to have more electrostatic repulsion against membrane surfaces than non-charged solutes. In particular, the operating parameters (Table 2) included the neutral pH range during the course of the SMBR operation. This indicates that all membrane surfaces possessed negative charges at the operating pH range and are electrostatically repulsive with negatively charged solutes. It is reported that hydrophobic particles in water influence the surface charge of the membrane [8]. The zeta potential of the membrane surface decreased due to the hydrophobic interactions between the membrane surface and hydrophobic particles compared to standard particles.

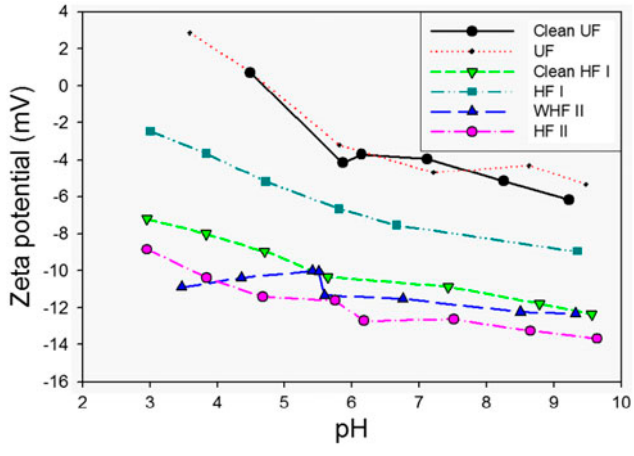

Fig. 1. Zeta potential distribution of membrane samples determined by streaming potential method as a function of pH.

3.1.2. Surface energies

A simple way to evaluate the adhesion between foulants and membrane can be calculated by work of adhesion [18]. If the contact angle value is small, the work of adhesion is large, and this is a more favourable condition for interactions between solutes and membrane surface. Contact angle values and calculated γ_S^{LW}, γ_S^+, γ_S^-, γ_S^{AB} and γ^{total} values of membrane samples are given in Table 5. The UF membranes used in this study were made of cellulose, and both the HF I and HF II membranes are made of PVDF. These distinctive material properties were expected to be reflected in different contact angles. However, overall contact angles were steady.

The effects of fouling on the contact angles of membrane surfaces were also insignificant. There were slight decreases in the water contact angles upon fouling formation, and this does not significantly change the total free energy of the surfaces (see Table 5). The overall surface free energy of the samples was not exceedingly high and was similar among membrane samples. It is also noted that the surface free energies of the membrane samples were dominated by Lifshitz–van der Waals intermolecular interactions, and there do not seem to be interactions with foulants via acid–base forces. The total surface free energies for membranes range from 59.0 to 64.5 mJ/m^2. Similarly to the zeta potential results, there was no significant difference between WHF II and HF II samples. Here, it was expected that the HF II membrane which was operated for longer time than the other membranes would exhibit more wetting and less hydrophobic properties and lower surface energy. However, contact angles, acid–base and total surface tensions for WHF II and HF II were almost steady and electron donor rich as shown in Table 5. The surface free energy of the UF membrane samples increased from 59.0 to 63.9 mJ/m^2 after deposition of the fouling layer. In contrast, HF I showed a lowered γ^{total} value after fouling formation from 64.5 to 61.4 mJ/m^2. This result was well correlated with the zeta potential results of HF I membranes, as the more the hydrophobic

Table 5
Contact angles of three probe liquids on membrane samples (W = water, G = glycerol and D = diiodomethane) and calculated γ_S^{LW}, γ_S^+, γ_S^-, γ_S^{AB} and γ^{total} values of membrane samples from the average of contact angle measurements

	W	G	D	γ_S^{LW}	γ_S^+	γ_S^-	γ_S^{AB}	γ^{total}
Clean UF	26.9 ± 2.3	18.0 ± 0.6	27.2 ± 2.3	45.3	1.3	45.3	13.7	59.0
UF	23.2 ± 1.4	12.3 ± 1.6	26.9 ± 2.3	50.8	1.3	41.6	13.1	63.9
Clean HF I	20.3 ± 1.5	23.3 ± 0.7	23.2 ± 1.3	50.8	0.7	46.2	13.7	64.5
HF I	18.6 ± 4.1	27.2 ± 3.1	21.7 ± 1.4	47.3	0.5	49.0	14.1	61.4
WHF II	26.9 ± 2.3	14.9 ± 0.1	22.3 ± 2.1	47.1	1.3	38.0	12.5	59.6
HF II	23.9 ± 1.9	11.7 ± 2.6	23.9 ± 0.8	46.5	1.3	40.1	12.9	59.4

Table 6
Amount of viable biomass in the fouling layers

Filtration mode	Membrane types	Biomass quantity (nmol/cm^2)
Passive filtration	UF	37.9
	HF I	31.8
Active filtration	WHF II	202.1
	HF II	249.2

surface, the more the negative zeta potential values [3], which suggests that after adsorption of biofoulants, it becomes more favourable for further biofilm development.

3.2. Biofouling under different filtration modes

Phospholipids are the main components of bacterial cell membranes up to 90–98% and remain stable in a wide range of stressed environment, and they have been widely adopted as an indicator of viable biomass [9,12,19]. Biomass consists of a biodegradable fraction and an inert fraction which is not degradable. The inert fraction is a combination of dead-end products and the extracellular matrix. The phospholipid is degradable which means that it can be useful as an assay for biofilm biomass estimation [11].

The results in Table 6 indicate similar rates of microbial biomass formation for the different membrane materials and structures (cellulose vs. PVDF and UF (flat sheet) vs. the HF I membrane) under the same foulants filtration mode. However, the different filtration modes (passive vs. active filtration) and operation time (2 weeks vs. 3 years) had a marked impact on the biofouling development. The biofouling on the membrane obtained by active filtration was more severe than that by passive filtration. The amount of biomass collected by active filtration was sevenfold higher than that by passive filtration. Microbial biomass in biofilms increased significantly with the age of the membranes and with operation mode from 31.8 and 37.9 nmol/cm^2 for HF I and UF membranes to 249.2 nmol/cm^2 for fouled HF II membrane, respectively (see Table 6). Given the higher amount of phospholipids in the WHF II samples as of 202.1 nmol/cm^2 compared to UF and HF I samples obtained by passive filtration, and little changes in the surface charges and energies between HF II and WHF II samples, it is evident that irreversible membrane biofouling occurred in the SMBR under active filtration mode. Even though the WHF II membrane was thoroughly washed, the amount of phospholipid was removed only 19% compared to HF II. Although there were no significant differences in electrostatic and hydrophobic membrane surface properties, the active filtration mode and longer filtration time have resulted in higher bioavailability and irreversible biofouling on the membrane surfaces.

4. Conclusions

In this study, the impacts of electrostatic and hydrophobic properties of membranes on biofouling were investigated. Membrane samples are negatively charged at all pHs, except for UF at pHs lower than 4.7. There was no indication of biofouling on membrane surfaces using zeta potential measurement except for HF I samples which showed distinctly different values of zeta potential between clean and fouled membrane samples. The surface energies of membranes were evaluated from detailed contact angle measurements. The total surface free energies of samples ranged from 59 to 65 mJ/m^2, and the surface

free energy was dominated by Lifshitz–van der Waals intermolecular interactions. Only HF I membranes showed positive correlation with zeta potential measurements favourable for further biofouling development. Phospholipids present on the membrane were quantified as a viable indicator of biofilm. Severe bifouling was observed on HF II membranes by means of lipid phosphate compared to other membrane samples. There were no positive correlations between total biomass assessment and surface energy or zeta potential measurements. However, active foulants filtration and prolonged operation both resulted in irreversible membrane biofouling in the SMBR.

Acknowledgements

This research was supported by a grant (15IFIP-B088091-02) from the Industrial Facilities & Infrastructure Research Program funded by Ministry of Land, Infrastructure and Transport of the Korean government. The authors also wish to thankfully acknowledge the support from the Korean Research Foundation and the UNESCO Centre for Membrane Science and Technology as the host institution for Youngpil Chun's Visiting Fellow appointment to conduct this research.

References

[1] P. Le-Clech, V. Chen, T.A.G. Fane, Fouling in membrane bioreactors used in wastewater treatment, J. Membr. Sci. 284 (2006) 17–53.
[2] Y. Miura, M.N. Hiraiwa, T. Ito, T. Itonaga, Y. Watanabe, S. Okabe, Bacterial community structures in MBRs treating municipal wastewater: Relationship between community stability and reactor performance, Water Res. 41 (2007) 627–637.
[3] M. Elimelech, W. Chen, J. Waypa, Measuring the zeta (electrokinetic) potential of reverse osmosis membranes by a streaming potential analyzer, Desalination 95 (1994) 269–286.
[4] Y. Chun, P.T. Ha, L. Powell, J. Lee, D. Kim, D. Choi, R.W. Lovitt, I.S. Kim, S.S. Mitra, I.S. Chang, Exploring microbial communities and differences of cartridge filters (CFs) and reverse osmosis (RO) membranes for seawater desalination processes, Desalination 298 (2012) 85–92.
[5] I. Kim, N. Jang, The effect of calcium on the membrane biofouling in the membrane bioreactor (MBR), Water Res. 40 (2006) 2756–2764.
[6] A. Drews, H. Evenblij, S. Rosenberger, Potential and drawbacks of microbiology-membrane interaction in membrane bioreactors, Environ. Prog. 24 (2005) 426–433.
[7] S. Xia, J. Guo, R. Wang, Performance of a pilot-scale submerged membrane bioreactor (MBR) in treating bathing wastewater, Bioresour. Technol. 99 (2008) 6834–6843.
[8] Y. Shim, H. Lee, S. Lee, S. Moon, J. Cho, Effects of natural organic matter and ionic species on membrane surface charge, Environ. Sci. Technol. 36 (2002) 3864–3871.
[9] P. Xu, C. Bellona, J.E. Drewes, Fouling of nanofiltration and reverse osmosis membranes during municipal wastewater reclamation: Membrane autopsy results from pilot-scale investigations, J. Membr. Sci. 353 (2010) 111–121.
[10] J.M. Veza, M. Ortiz, J.J. Sadhwani, J.E. Gonzalez, F.J. Santana, Measurement of biofouling in seawater: Some practical tests, Desalination 220 (2008) 326–334.
[11] C. Arnaiz, J.C. Gutierrez, J. Lebrato, Support material selection for anaerobic fluidized bed reactors by phospholipid analysis, Biochem. Eng. J. 27 (2006) 240–245.
[12] R.H. Findlay, G.M. King, L. Watling, Efficacy of phospholipid analysis in determining microbial biomass in sediments, Appl. Environ. Microbiol. 55 (1989) 2888–2893.
[13] F. Fairbrother, H. Mastin, CCCXII.—Studies in electro-endosmosis. Part I, J. Chem. Soc. Trans. 125 (1924) 2319–2330.
[14] E. McCafferty, Acid-base effects in polymer adhesion at metal surfaces, J. Adhes. Sci. Technol. 16 (2002) 239–255.
[15] C. Oss, Interfacial Forces in Aqueous Media, vol. 440, Marcel Decker, New York, NY, 1994.
[16] P.G. de Gennes, Wetting: Statics and dynamics, Rev. Mod. Phys. 57 (1985) 827–863.
[17] Q. Zhao, C. Wang, Y. Liu, S. Wang, Bacterial adhesion on the metal-polymer composite coatings, Int. J. Adhes. Adhes. 27 (2007) 85–91.
[18] S. Bargir, S. Dunn, B. Jefferson, J. Macadam, S. Parsons, The use of contact angle measurements to estimate the adhesion propensity of calcium carbonate to solid substrates in water, Appl. Surf. Sci. 255 (2009) 4873–4879.
[19] D.C. White, W.M. Davis, J.S. Nickels, J.D. King, R.J. Bobbie, Determination of the sedimentary microbial biomass by extractible lipid phosphate, Oecologia 40 (1979) 51–62.